

An Analytical Approach to Operational Space Control of Robotic Manipulators with Kinematic Constraints^{*}

Cong Dung Pham^{*} Fernando Coutinho^{**} Fernando Lizarralde^{**}
Liu Hsu^{**} Pål Johan From^{*}

^{*} Department of Mathematical Sciences and Technology,
Norwegian University of Life Sciences, 1432 Ås, Norway.

^{**} Department of Electrical Engineering - COPPE, Federal University of Rio
de Janeiro, Rio de Janeiro, 21945/970 RJ, Brazil

Abstract:

This paper presents a novel control architecture for operational space control when the end effector or the robotic chain is kinematically constrained. Particularly, we address kinematic control of robots operating in the presence of obstacles such as point, plane, or barrier constraints imposed on a point on the manipulator. The main advantage of the proposed approach is that we are able to control the end-effector motion in the normal way using conventional operational space control schemes, and by re-writing the Jacobian matrix we also guarantee that the constraints are satisfied. The most challenging problem of obstacle avoidance of robotic manipulators is the extremely complex structure that arises when the obstacles are mapped from the operational space to joint space. We solve this by first finding a new set of velocity variables for a point on the robot in the vicinity of the obstacle, and on these new variables we impose a structure which guarantees that the robot does not hit the obstacle. We then find a mapping denoted the Constrained Jacobian Matrix from the joint variables to these new velocity variables and use this mapping to find a trajectory in joint space for which the constraints are not violated. We present for the first time the Constrained Jacobian Matrix which imposes a kinematic constraint on the manipulator chain and show the efficiency of the approach through experiments on a real robot.

Keywords: Robotic Manipulators, Robot Kinematics, Jacobian Matrices, Redundant Manipulators.

1. INTRODUCTION

Efficient solutions to collision avoidance for complex kinematic chains in the presence of obstacles of different shape and form is an extremely challenging problem. The obstacles impose constraints of different shape and dimension on one or several points on the kinematic chain which results in very complex kinematics when the constraints are taken into account. Particularly, the mapping from the joint velocities to the end-effector velocities cannot be found in the standard way by the manipulator Jacobian when constraints are present.

The main objective of robot control, whether the trajectory is computer generated or given by an operator through a haptic device, is to control the end-effector motion to achieve a certain task or obtain a desired behavior. The control signal sent to the robot is therefore often a joint velocity reference calculated from the desired end-effector velocity by the inverse of the Jacobian matrix. This mapping does not, however, take into account the constraints imposed by obstacles in the robot's workspace. In this paper we thus propose a *Constrained Jacobian Matrix (CJM)* that maps the joint velocities to the end-effector velocities *subject to the constraints imposed by the obstacles*. The Constrained Jacobian Matrix gives us a velocity

reference for the joints which guarantees that the constraints are not violated.

In this paper we solve the constrained kinematics problem by first defining a new set of velocity variables from the desired end-effector velocity in such a way that the reduced dimensionality due to the constraints are cast into the velocity variables by imposing a certain structure on these new variables. The velocity variables define a motion of a point on the robot that is close to the obstacle and the new structure guarantees that the constraints imposed by the obstacle are obtained. Secondly, we find the Jacobian matrix, denoted the Constrained Jacobian Matrix, which maps the *new* velocity variables into the joint velocities, and thus allows us to find a *trajectory in joint space for which the constraints are not violated*. Finally the control is obtained in the standard way by replacing the standard Jacobian matrix with the Constrained Jacobian Matrix. Early results were presented in From [2013]. In this paper we present for the first time the Constrained Jacobian Matrix when the constraints are imposed on a point on the kinematic chain and verify the formulation empirically.

As the main control objective of the great majority of the applications found in robotics is to obtain a desired behavior of the tool, the control law needs to be defined in the operational space. We thus require a framework which allows the control law to be formulated in the end-effector frame and at the same time satisfies the kinematic constraints defined in the inertial

^{*} During this work, P. J. From and C. D. Pham were visiting the Department of Electrical Engineering - COPPE, Federal University of Rio de Janeiro, Rio de Janeiro, 21945/970 RJ, Brazil.

frame. The Constrained Jacobian Matrix allows us to derive such a control law because it maps the joint velocities to the end-effector velocities subject to the constraints imposed on the robot.

Defining the control law in the end-effector frame allows us to apply control schemes such as impedance and hybrid control in the tool frame. Hybrid control in the end-effector space has been studied in detail by many authors and lets the end-effector space be divided into directions which require stiff control and directions that require soft compliant control (Natale [2003], Mason [1981], Craig and Raibert [1979], Abbati-Marescotti et al. [1990], Bruyninckx and De Schutter [1996], Lipkin and Duffy [1988]). One example in which hybrid or compliant control is required at the end effector and for which the kinematic chain is constrained is Robotics-assisted Minimally Invasive Surgery (RAMIS). The constraints imposed by the entry point where the robot enters the human body require zero lateral velocity in order to not damage the patient (Funda et al. [1996], Li et al. [2005], Ortmaier and Hirzinger [2000], Locke and Patel [2007], Lenarčič and Galletti [2004], Azimian et al. [2010]). Other examples are robot manipulators in a cluttered environment or mobile manipulators for which the mobile base needs to avoid hitting obstacles while following a desired trajectory for the end effector.

The paper is organized as follows: In Section 3 and 4 we present the overall idea of how the kinematics of a constrained kinematic chain is calculated. The mathematical representation of the different kinematic constraints are presented in Section 5 and the corresponding Jacobian matrices are found in Section 6. A simple study case with constraints on the chain is presented in Section 7 where we also show how the results from Sections 5 and 6 are used and how the calculations are carried out in practice. The experimental results are presented in Section 8 and the relevant research and concluding remarks are presented in Sections 2 and 9, respectively.

2. RELATED RESEARCH

The motion planning problem has been studied by several researchers over the last decades and a wide variety of approaches have been developed to solve this problem. In general the problem is quite different for mobile robots and robotic manipulators. For mobile robots the motion planning problem normally reduces to finding a point trajectory in a cluttered environment. Even though the problem is easy to formulate it has shown to be a difficult problem to solve and still remains an active area of research. However, several results have been obtained over the last three-four decades for efficient obstacle avoidance of mobile robots. For robotic manipulators on the other hand, the complex kinematics, the collision avoidance of several bodies, and in particular the complex geometry of the obstacles when mapped to the high-dimensional joint space make motion planning extremely hard to solve.

Motion planning for vehicles and mobile robots is the problem of finding a continuous path from an initial to a final position and orientation without colliding with objects in the robot's workspace. This problem is very simple to formulate, but has turned out to be rather difficult to solve. The very first attempts to solve this problem use the notion of configuration space (Lozano-Perez [1983], Siciliano et al. [2011]) and use roadmaps to connect the initial and final position through collision-free paths. Generalized Veroni diagrams can be used

efficiently to solve this problem in an optimal manner in the sense that the distance to the obstacles is minimized (ODunlaing and Yap [1985]). Another early approach decomposes the collision-free workspace into cells and then find a collision-free path by connecting the cells so that a collision-free path from the initial to the final position is found (Schwartz and Sharir [1983a,b]). We refer to LaValle [2006], Canny [1988] and Latombe [1991] for more details on motion planning of mobile robots and vehicles.

In the case of robotic manipulators the problem of obstacle avoidance is normally solved by introducing a potential field pushing the manipulator away from the obstacle (Khatib [1986]). Normally two types of potential fields are applied to the robot: i) an attractive potential U_a that pushes the robot end effector towards its desired position and a repulsive field U_{ri} that pushes each link of the robot and the robot end effector away from the obstacles. The total potential field is given by

$$U_t = U_a + \sum U_{ri} \quad (1)$$

which can be realized either as a joint torque

$$\tau_t = -(J_e^S(q))^T \Delta U_t(p_e) - \sum (J_i^S(q))^T \Delta U_t(p_i) \quad (2)$$

or as joint velocity

$$\dot{q}_t = -(J_e^S(q))^T \Delta U_t(p_e) - \sum (J_i^S(q))^T \Delta U_t(p_i) \quad (3)$$

where p_i for $i = 1, \dots, m$ are the points of the manipulator that are checked for collision and J_i^S is the Jacobian matrix of the same points. The main advantage of Equation (2) is smooth motion obtained as the forces are filtered through the manipulator dynamics. Equation (3), on the other hand, has a quicker response and responds quicker to trajectory errors or moving objects.

We see that the potential field in principle guarantees that the robot does not hit the obstacles, as the artificial force pushes the robot away from the obstacle with a higher force as the distance to the obstacle reduces. Although the strength of the potential field can be tuned, the formulation does not allow for exact positioning of the robot with respect to the obstacles. For more complex obstacles like holes and planes we need to be able to position the robot more accurately in the presence of the obstacle which calls for an analytical approach to the problem. Furthermore, obstacles such as forcing a point to lie between two planes are not solved very efficiently by potential fields as they require two potential fields pushing in opposite directions which may cause unstable and oscillating behavior. When several forces are present these can also eliminate each other and the robot can encounter local minima in which it gets blocked.

3. SYSTEM OVERVIEW AND PROBLEM FORMULATION

The system discussed in this paper consists of a redundant robotic manipulator in the presence of obstacles. The redundancy is obtained either by placing a standard manipulator on a moving base, by utilizing a manipulator with a higher mobility than the task space, or a combination of these. At some given points in the Cartesian space we will require that the velocities of the links are eliminated in certain directions to prevent the robot from hitting an obstacle. The system setup together with the most important configuration spaces used in this paper are shown in Fig. 1. We denote the frame of the joint located before

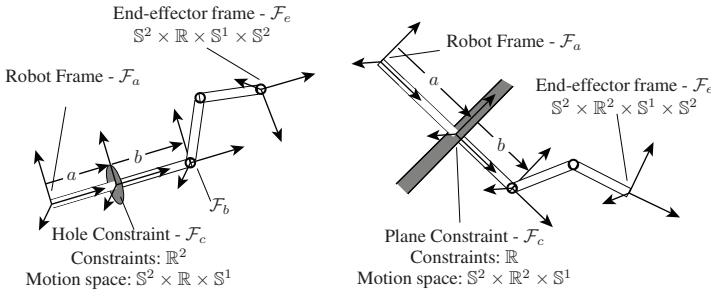


Fig. 1. Two examples of the constraints discussed in this paper: on the left, a hole constraint which prevents any lateral motion of a specific point on the manipulator chain; and on the right, a plane constraint that restricts the linear motion of a point to a given direction in the plane. The constrained link is constrained at the point \mathcal{F}_c which in turn results in a reduced motion space at \mathcal{F}_a . The motion spaces of the different frames are subgroups of $SE(3)$ defined by linear motion \mathbb{R} , circular motion \mathbb{S} , and the sphere \mathbb{S}^2 .

the constraint located at \mathcal{F}_c in the chain by \mathcal{F}_a and the joint that is located after the constraint is denoted \mathcal{F}_b . The desired end-effector motion is given by the frame \mathcal{F}_e . We will denote the velocity variables in the following way

$$V_{0e}^{B,S} = [v_x^e \ v_y^e \ v_z^e \ \omega_x^e \ \omega_y^e \ \omega_z^e]^T \quad (4)$$

and similarly for the other frames. $V_{ij}^{B,S}$ is thus the velocity in body or spatial coordinates of a rigid body with frame \mathcal{F}_j with respect to the frame \mathcal{F}_i . V_{ij}^B is an element of the Lie algebra $se(3)$ of the Special Euclidean Group $SE(3)$, and is found as $V_{ij}^B = g_{ij}^{-1} \dot{g}_{ij}$ where g_{ij} is the homogeneous transformation matrix describing the location of \mathcal{F}_j in \mathcal{F}_i .

The problem considered consists of maintaining a stiff control of zero velocity in certain directions in the presence of obstacles while the end effector follows the desired trajectory. The objective is to obtain a formulation that allows us to control the end effector using any of the conventional control schemes without violating the constraints. The approach should thus allow for control schemes such as trajectory following, impedance control, or a combination of stiff and compliant control of the end effector. Common for all these control schemes is that a formulation which allows the controller to act on the end effector variables directly is required, and not for example on the joint variables.

4. CONSTRAINED KINEMATICS

The overall goal of this paper is to derive the motion of a kinematic chain given a desired end-effector motion \mathcal{F}_e and a kinematic constraint at a point represented by \mathcal{F}_c . In the next sections we will find the admissible velocities at \mathcal{F}_c for different types of constraints and the corresponding admissible velocities at the last joint prior to the constrained link, i.e., at \mathcal{F}_a . In this section we will present the overall idea of how these relations are used to find the kinematics of a constrained kinematic chain.

The main idea is to find the velocity V_{0a}^B in terms of a set of new velocity variables parametrized in such a way that these variables can be chosen freely and at the same time guarantee that the constraints at \mathcal{F}_c are satisfied. This means that certain directions in the velocity space are reduced from a higher to a lower-dimensional space represented by new velocity variables v_i .

As our main objective is to follow a desired end-effector motion V_{0e}^B we need to find the mapping from V_{0e}^B to the free variables, i.e., V_{0a}^B with the reduction in dimensionality represented by v_i . This is obtained in the following way:

- (1) Define a desired end-effector velocity V_{0e}^B .
- (2) Given a constraint at \mathcal{F}_c , define the velocities at this point which satisfy the constraints, i.e., the velocities at the previous joint \mathcal{F}_a are given by
 - the free variables $\{v_x^a, v_y^a, v_z^a, \omega_x^a, \omega_y^a, \omega_z^a\}$, and
 - the constrained variables $\{v_1, v_2, v_3, \dots\}$.

The free variables are the ones that can be chosen freely and do not affect the constraint. The constraint variables require a specific form and structure for the constraints to be satisfied. We therefore replace some of the free variables with the constraint variables which gives us the required structure. These variables thus represent a freedom, but in a space with reduced dimensionality that satisfies the constraint. The constrained variables are thus written in terms of the free variables v as

$$V_{0a}^B = V_{0a}^B(v). \quad (5)$$

- (3) Eliminate the redundant variables that arise as a result of the reduced dimensionality and denote the minimal representation of the velocity variables by \bar{V}_{0a}^B .
- (4) Find a mapping from the end-effector velocities V_{0e}^B to the new reduced velocity variables \bar{V}_{0a}^B , which take the form

$$v_m^a = \begin{bmatrix} \bar{V}_{0a}^B \\ \dot{q} \end{bmatrix} = \begin{bmatrix} \text{constrained variables} \\ \text{free variables} \\ \text{joint velocities} \end{bmatrix}. \quad (6)$$

The mapping is given by the Constrained Jacobian Matrix J_{ea}^m that gives the important relation $V_{0e}^B = J_{ea}^m v_m^a$, i.e., the transformation from the new reduced velocity variables v_m^a to the desired end-effector velocities V_{0e}^B .

The *joint velocities* represent the joints that are determined by the end-effector velocity V_{0e}^B only and do not depend on the constraints. These are typically the joints that are situated between the constraint and the end effector. The *free variables* are the velocities of \mathcal{F}_a that do not depend on the constraint, but differently from the *joint velocities*, they depend on the joints between the base and the constraint. Finally, the *constrained variables* are constraint dependent and give the velocity at \mathcal{F}_a the required structure so that the constraints are satisfied.

- (5) From the new variables, find the robot velocity at \mathcal{F}_a .

We note that there are two main steps. Firstly, we need to find a suitable representation of the velocity variables, which is discussed in Section 5. Secondly, we need to define the Constrained Jacobian Matrix, which treated in Section 6.

5. CONSTRAINT KINEMATICS

In this section we derive the kinematics of the constraints. This is used in the next section to derive the constrained kinematics of the robotic manipulator in the velocity space, i.e., the Constrained Jacobian Matrix.

5.1 Plane Constraint

For a plane-shaped constraint we want to eliminate the velocity at \mathcal{F}_c in one direction. Lets assume that we allow no velocity in the direction of v_y^c . As this can be written in terms of the velocities at \mathcal{F}_a (prior to the entry point) as

$$v_y^c = v_y^a - a\omega_x^a \quad (7)$$

the constraint $v_y^c = 0$ can be transformed to the frame \mathcal{F}_a as

$$v_y^a = a\omega_x^a. \quad (8)$$

We can now introduce a new variable v_1 which describes the one degree of freedom represented by (8). The constrained variables v_y^a and ω_x^a then take the form

$$v_y^a = v_1 \quad \omega_x^a = \frac{1}{a}v_1 \quad (9)$$

which forces a point \mathcal{F}_c on the robot to avoid lateral motion in the direction of the y -axis. The constrained velocity variables at \mathcal{F}_a can now be written as

$$\begin{bmatrix} v_x^a \\ v_y^a \\ v_z^a \\ \omega_x^a \\ \omega_y^a \\ \omega_z^a \end{bmatrix} = \begin{bmatrix} v_x^a \\ v_1 \\ v_z^a \\ \frac{1}{a}v_1 \\ \omega_y^a \\ \omega_z^a \end{bmatrix} \quad (10)$$

which have five degrees of freedom, as expected. We see that we impose a certain structure on the velocities at \mathcal{F}_a which guarantees that the constraints are satisfied.

5.2 Entry Hole

Assume a robotic chain that is inserted through a hole. This add a 2-DoF constraint to the point of entry, represented by \mathcal{F}_c , which is a point on the link penetrating the hole. This is for example the case in minimally invasive surgery where the robot is to be inserted into the abdomen through a trocar.

Similarly with Section 5.1, we can incorporate these constraints in the kinematics by introducing new variables v_1 and v_2 such that

$$v_x^a = v_1 \quad \omega_y^a = -\frac{1}{a}v_1 \quad (11)$$

$$v_y^a = v_2 \quad \omega_x^a = \frac{1}{a}v_2 \quad (12)$$

which for any choice of v_1 and v_2 will result in zero lateral velocity at the entry point. The constrained velocities can now be given as

$$\begin{bmatrix} v_x^a \\ v_y^a \\ v_z^a \\ \omega_x^a \\ \omega_y^a \\ \omega_z^a \end{bmatrix} = \begin{bmatrix} v_1 \\ v_2 \\ v_z^a \\ \frac{1}{a}v_2 \\ \frac{1}{a} \\ -\frac{1}{a}v_1 \\ \omega_z^a \end{bmatrix}. \quad (13)$$

The expressions are found similarly for other types of constraints.

6. CONSTRAINED JACOBIAN MATRIX

In this section we will find the relation between the desired end-effector velocities and the corresponding joint velocities subject to the constraints described in the previous section. Given the end-effector velocity we want to find the free and constrained velocity variables of the robot. We will find the Constrained Jacobian Matrix J_{ea}^m which gives the relation $V_{0e}^B = J_{ea}^m v_m^a$ and the required velocities v_m^a are found from the desired end-effector velocities by the inverse of the Constrained Jacobian Matrix.

The standard body Jacobian matrix gives the mapping from the joint velocities to the end-effector velocities in body coordinates and is given by (From et al. [2014])

$$J_e^B = [X_1^\dagger \ X_2^\dagger \ \dots \ X_n^\dagger] \quad (14)$$

$$= [\text{Ad}_{g_{1e}}^{-1} X_1^\dagger \ \text{Ad}_{g_{2e}}^{-1} X_2^\dagger \ \dots \ X_n^\dagger] \in \mathbb{R}^{n \times 6}$$

where X_i^i is the constant twist in frame \mathcal{F}_i and $\text{Ad}_{g_{ie}}^{-1}$ is the Adjoint matrix that transforms X_i^i from frame \mathcal{F}_i to X_i^\dagger represented in the end-effector frame \mathcal{F}_e . The body Jacobian matrix can also be found for other links than the end effector, in which case it is denoted J_i^B which gives the velocities of link i . Particularly, the Jacobian matrix that gives the velocity of the link \mathcal{F}_a located before the constraint is denoted J_a^B .

In this section we will find the body Jacobian matrices, as above, but subject to the constraints, i.e., we find the mapping from the joint velocity variables to the respective links subject to a constraint on the velocity at the constraint frame \mathcal{F}_c . We will see that for a large class of constraints the Constrained Jacobian Matrix can be written in the form

$$\bar{J}_a^B = \left[\sum \alpha_i X_i^\dagger \ \sum \alpha_j X_j^\dagger \ \dots \ \sum \alpha_k X_k^\dagger \right] \in \mathbb{R}^{m \times 6} \quad (15)$$

for some $(n - m)$ -dimensional constraint. Where the bar in \bar{J}_a^B distinguishes the Constrained Jacobian Matrix from the standard Jacobian J_a^B . X_i^\dagger are the manipulator twists while α_i are configuration-dependent functions of the manipulator and constraint kinematics. The form of the Constrained Jacobian Matrix depends on the type of constraint. We will now look at what the constrained Jacobian matrices look like for different types of constraints.

6.1 Plane Constraint

Following the approach in From [2013] we see from (10) that the Constrained Jacobian Matrix can be found by adding columns two and four of the standard Jacobian, i.e.,

$$\bar{J}_a^B = \left[\sum \alpha_i X_i^\dagger \ \sum \alpha_j X_j^\dagger \ \dots \ \sum \alpha_k X_k^\dagger \right]$$

$$= \left[X_1^\dagger \ X_2^\dagger + \frac{1}{a}X_4^\dagger \ X_3^\dagger \ X_5^\dagger \ X_6^\dagger \ X_7^\dagger \right] \in \mathbb{R}^{6 \times 6}. \quad (16)$$

For a manipulator like the one in Fig. 1 with one joint after the constraint the required expression is given by the expression $V_{0e}^B = \bar{J}_a^B v_m^a$ which is found as

$$V_{0e}^B = \text{Ad}_{g_{eb}} V_{0b}^B + V_{be}^B \quad (17)$$

with

$$\text{Ad}_{g_{eb}} = \text{Ad}_{g_{be}^{-1}} = \begin{bmatrix} R_{be}^\top & -R_{be}^\top \hat{p}_{be} \\ 0 & R_{be}^\top \end{bmatrix}$$

$$= \begin{bmatrix} 1 & 0 & 0 & 0 & l_7 c q_7 & l_7 s q_7 \\ 0 & c q_7 & s q_7 & -l_7 & 0 & 0 \\ 0 & -s q_7 & c q_7 & 0 & 0 & 0 \\ 0 & 0 & 0 & 1 & 0 & 0 \\ 0 & 0 & 0 & 0 & c q_7 & s q_7 \\ 0 & 0 & 0 & 0 & -s q_7 & c q_7 \end{bmatrix} \quad (18)$$

$$V_{0b}^B = \begin{bmatrix} 1 & 0 & 0 & 0 & (a+b) & 0 \\ 0 & 1 & 0 & -(a+b) & 0 & 0 \\ 0 & 0 & 1 & 0 & 0 & 0 \\ 0 & 0 & 0 & 1 & 0 & 0 \\ 0 & 0 & 0 & 0 & 1 & 0 \\ 0 & 0 & 0 & 0 & 0 & 1 \end{bmatrix} \begin{bmatrix} v_x^a \\ v_1 \\ v_z^a \\ \frac{1}{a}v_1 \\ a \\ \omega_z^a \end{bmatrix} \quad (19)$$

$$V_{be}^B = \begin{bmatrix} 0 \\ -l_7 \\ 0 \\ 1 \\ 0 \\ 0 \end{bmatrix} \dot{q}_7. \quad (20)$$

so that $V_{0e}^B = \bar{J}_a^B v_m^a$ can be written as

$$V_{0e}^B = \begin{bmatrix} 1 & 0 & 0 & \beta_1 + l_7 c q_7 & l_7 s q_7 & 0 \\ 0 & \alpha_1 & s q_7 & 0 & 0 & -l_7 \\ 0 & \frac{b}{a} s q_7 & c q_7 & 0 & 0 & 0 \\ 0 & \frac{1}{a} & 0 & 0 & 0 & 1 \\ 0 & \frac{a}{a} & 0 & c q_7 & s q_7 & 0 \\ 0 & 0 & 0 & -s q_7 & c q_7 & 0 \end{bmatrix} \begin{bmatrix} v_x^a \\ v_y^a \\ v_z^a \\ \omega_x^a \\ \omega_y^a \\ \omega_z^a \end{bmatrix} \quad (21)$$

where we have defined $\alpha_1 = -\frac{b}{a} \cos q_7 - \frac{1}{a} l_7$ and $\beta_1 = (a+b)$.

The new velocity variables are then found from the inverse of this expression as

$$v_m^a = (\bar{J}_a^B)^{-1} V_{0e}^B. \quad (22)$$

6.2 Entry Hole

Similarly, the Constrained Jacobian Matrix can be found as

$$\bar{J}_a^B = \left[X_1^\dagger - \frac{1}{a} X_5^\dagger \quad X_2^\dagger + \frac{1}{a} X_4^\dagger \quad X_3^\dagger \quad X_6^\dagger \quad X_7^\dagger \quad X_8^\dagger \right] \in \mathbb{R}^{6 \times 6} \quad (23)$$

for a hole-shaped constraint. We have

$$V_{0e}^B = \text{Ad}_{g_{eb}} V_{0b}^B + V_{be}^B \quad (24)$$

which for a robot like the one in Fig. 1 with two joints after the constraint gives

$$\begin{aligned} \text{Ad}_{g_{eb}} &= \text{Ad}_{g_{be}^{-1}} = \begin{bmatrix} R_{be}^\top & -R_{be}^\top \hat{p}_{be} \\ 0 & R_{be}^\top \end{bmatrix} \\ &= \begin{bmatrix} 1 & 0 & 0 & 0 & l_7 c q_7 & l_7 s q_7 \\ 0 & c q_7 s & s q_7 s & -l_7 c q_8 & 0 & 0 \\ 0 & -s q_7 s & c q_7 s & l_7 s q_8 & 0 & 0 \\ 0 & 0 & 0 & 1 & 0 & 0 \\ 0 & 0 & 0 & 0 & c q_7 s & s q_7 s \\ 0 & 0 & 0 & 0 & -s q_7 s & c q_7 s \end{bmatrix} \end{aligned} \quad (25)$$

$$V_{0b}^B = \begin{bmatrix} 1 & 0 & 0 & 0 & (a+b) & 0 \\ 0 & 1 & 0 & -(a+b) & 0 & 0 \\ 0 & 0 & 1 & 0 & 0 & 0 \\ 0 & 0 & 0 & 1 & 0 & 0 \\ 0 & 0 & 0 & 0 & 1 & 0 \\ 0 & 0 & 0 & 0 & 0 & 1 \end{bmatrix} \begin{bmatrix} v_1 \\ v_2 \\ v_z^a \\ \frac{1}{a} v_2 \\ a_1 \\ -\frac{1}{a} v_1 \\ \frac{a}{a} \\ \omega_z^a \end{bmatrix} \quad (26)$$

$$V_{be}^B = \begin{bmatrix} 0 & 0 \\ -l_7 c q_8 & 0 \\ l_7 s q_8 & 0 \\ 1 & 1 \\ 0 & 0 \\ 0 & 0 \end{bmatrix} \begin{bmatrix} \dot{q}_7 \\ \dot{q}_8 \end{bmatrix} \quad (27)$$

The expression $V_{0e}^B = \bar{J}_a^B v_m^a$ is found as

$$\begin{bmatrix} v_x^e \\ v_y^e \\ v_z^e \\ \omega_x^e \\ \omega_y^e \\ \omega_z^e \end{bmatrix} = \begin{bmatrix} -\alpha_1 & 0 & 0 & l_7 s q_7 & 0 & 0 \\ 0 & -\beta_1 & s q_7 s & 0 & -l_7 c q_8 & 0 \\ 0 & \beta_2 & c q_7 s & 0 & l_7 s q_8 & 0 \\ 0 & \frac{1}{a} & 0 & 0 & 1 & 1 \\ -\frac{1}{a} c q_7 s & 0 & 0 & s q_7 s & 0 & 0 \\ \frac{1}{a} s q_7 s & 0 & 0 & c q_7 s & 0 & 0 \end{bmatrix} \begin{bmatrix} v_1 \\ v_2 \\ v_z^a \\ \omega_z^a \\ \dot{q}_7 \\ \dot{q}_8 \end{bmatrix}. \quad (28)$$

Here we have defined $\alpha_1 = \frac{1}{a}(b+l_7 c q_7)$, $\beta_1 = \frac{1}{a}(b c q_7 s + l_7 c q_8)$ and $\beta_2 = \frac{1}{a}(b s q_7 s + l_7 s q_8)$.

7. CASE STUDY - HOLE CONSTRAINT ON THE CHAIN

We will see how the calculations are carried out through a simple example.

Assume a robotic manipulators as the one pictured to the left in Fig. 1 with 6 degrees of freedom before and another 2 degrees of freedom after the constraint. Assume further that the constraint is a hole, i.e., a 2-DoF constraint given by (13). The kinematic relations are then found as follows:

- (1) The end-effector velocity is given by V_{0e}^B .
- (2) The lateral velocities at \mathcal{F}_c are required to be zero, which for our choice of reference frame gives $v_x^c = v_y^c = 0$. The corresponding velocities at \mathcal{F}_a are then found as

$$\begin{bmatrix} v_x^a \\ v_y^a \\ v_z^a \\ \omega_x^a \\ \omega_y^a \\ \omega_z^a \end{bmatrix} = \begin{bmatrix} v_1 \\ v_2 \\ v_z^a \\ \frac{1}{a} v_2 \\ a_1 \\ -\frac{1}{a} v_1 \\ \frac{a}{a} \\ \omega_z^a \end{bmatrix}. \quad (29)$$

- (3) The reduced variables are then found by eliminating the dependent variables ω_x^a and ω_y^a :

$$\bar{V}_{0a}^B = \begin{bmatrix} v_1 \\ v_2 \\ v_z^a \\ \omega_z^a \end{bmatrix}. \quad (30)$$

- (4) The mapping from the end-effector velocities to these new velocity variables can now be found as

$$\begin{bmatrix} v_x^e \\ v_y^e \\ v_z^e \\ \omega_x^e \\ \omega_y^e \\ \omega_z^e \end{bmatrix} = \begin{bmatrix} -\alpha_1 & 0 & 0 & l_7 s q_7 & 0 & 0 \\ 0 & -\beta_1 & s q_7 s & 0 & -l_7 c q_8 & 0 \\ 0 & \beta_2 & c q_7 s & 0 & l_7 s q_8 & 0 \\ 0 & \frac{1}{a} & 0 & 0 & 1 & 1 \\ -\frac{1}{a} c q_7 s & 0 & 0 & s q_7 s & 0 & 0 \\ \frac{1}{a} s q_7 s & 0 & 0 & c q_7 s & 0 & 0 \end{bmatrix} \begin{bmatrix} v_1 \\ v_2 \\ v_z^a \\ \omega_z^a \\ \dot{q}_7 \\ \dot{q}_8 \end{bmatrix}. \quad (31)$$

We see that we have found a mapping from the 6-DoF end-effector space to the another 6-DoF space represented by a 6-DoF manipulator, a 2-DoF wrist and a 2-DoF hole constraint.

This is suitable for workspace control and at the same time guarantees that the entry point velocity constraints are satisfied.

- (5) Finally the robot velocities are found from Equations (11-12) as

$$\begin{bmatrix} v_x^a \\ v_y^a \\ v_z^a \\ \omega_x^a \\ \omega_y^a \\ \omega_z^a \end{bmatrix} = \begin{bmatrix} 1 & 0 & 0 & 0 \\ 0 & 1 & 0 & 0 \\ 0 & 0 & 1 & 0 \\ 0 & \frac{1}{a} & 0 & 0 \\ -\frac{1}{a} & 0 & 0 & 0 \\ 0 & 0 & 0 & 1 \end{bmatrix} \begin{bmatrix} v_1 \\ v_2 \\ v_z^a \\ \omega_z^a \end{bmatrix} \quad (32)$$

and the corresponding joint velocities are found from the manipulator Jacobian in the standard way and fed to the controller together with the joint velocities found in point (4).

7.1 Singularity Avoidance

We cannot, in general, guarantee that there exists a set of joint velocities v_m^a which generates the desired end-effector velocities V_{0e}^B . For instance, if the Constrained Jacobian Matrix \bar{J}_a^B is singular, the end-effector motion cannot be generated.

The damped least square (DLS) method to avoid singularities for the manipulator Jacobian J_a^B can be written as (Siciliano et al. [2011]).

$$V_{0e}^B = (J_a^B)^T \left(J_a^B (J_a^B)^T + \lambda^2 I \right)^{-1} \dot{q}. \quad (33)$$

We can use the same idea to avoid singularities in the CJM. Assume that we want to minimize the cost function

$$f(v_m^a) = \|\bar{J}_a^B v_m^a - V_{0e}^B\| + \lambda^2 \|v_m^a\| \quad (34)$$

We can rewrite this as

$$\begin{aligned} \left\| \begin{bmatrix} \bar{J}_a^B \\ 0 \end{bmatrix} v_m^a - \begin{bmatrix} V_{0e}^B \\ 0 \end{bmatrix} \right\| &= 0 \\ \begin{bmatrix} (\bar{J}_a^B)^T & \lambda I \end{bmatrix} \begin{bmatrix} \bar{J}_a^B \\ \lambda I \end{bmatrix} v_m^a &= \begin{bmatrix} (\bar{J}_a^B)^T & \lambda I \end{bmatrix} \begin{bmatrix} V_{0e}^B \\ 0 \end{bmatrix} \\ ((\bar{J}_a^B)^T \bar{J}_a^B + \lambda^2 I) v_m^a &= (\bar{J}_a^B)^T V_{0e}^B \\ v_m^a &= (\bar{J}_a^B)^T \left(\bar{J}_a^B (\bar{J}_a^B)^T + \lambda^2 I \right)^{-1} V_{0e}^B. \end{aligned} \quad (35)$$

Our DLS has the same form as for the standard approach, but the interpretation is somewhat different. We restrict the velocities in the new variables v_m^a while following the desired end effector trajectory V_{0e}^B as tightly as possible, which differs from the standard formulation which restrict the joint velocities directly. We thus avoid the singularities that arise as a result of the constraints imposed on the chain, and not the kinematic singularities of the robot arm itself.

8. EXPERIMENTS

To verify the proposed theory a simple setup with a manipulator was used.

8.1 Experimental Setup

To verify this theory, we control a manipulator by a haptic device. A standard 6-DoF Phantom haptic device from Sensable was used to control a Motoman DIA-10, which is a dual-arm robot. Each arm on the Motoman DIA-10 has 7 axes of motion and a "human-like" structure. The robot also has a 1-DoF base. We want the robot end effector to follow the reference, so workspace control is required. The time delay is minimal and not treated in this paper. The control is, however, implemented so that it is robust with respect to time delays.



Fig. 2. The robot and the constraint

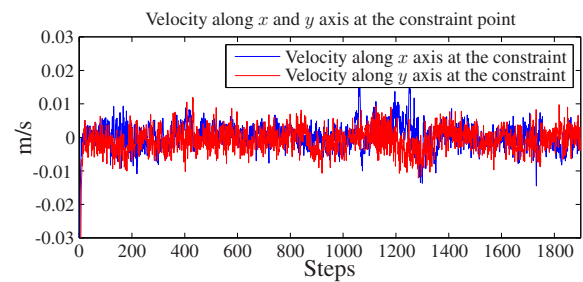


Fig. 3. Velocity along x and y axis at the constraint point

8.2 Experimental Results

The end effector of the Motoman is to follow the reference from the master without violating the constraint. We use one arm of the Motoman and the base so the arm has 8 degrees of freedom. We apply the hole constraint on link 6. So we have 6 degrees of freedom before the constraint and 2 degrees of freedom after the constraint.

The velocities at the constraint are shown in Fig. 3. We can see the velocities v_x^c and v_y^c along x - and y -axes, respectively, that are, except for the noise, very close to zero, which shows that the entry point constraint is satisfied.

In Fig. 4, we see how well the actual velocities at the end effector follow the desired velocities. From Fig. 3 and Fig. 4, we can conclude that our manipulator satisfies the constraint while the end effector still follow the desired values. The variances of the velocities at the constraint and the end effector are calculated to approximately $2 \cdot 10^{-6}$ so we conclude that this is noise in both cases.

An illustration of the robot showing overlaid images is shown in Fig. 2. We see that for a single point on the arm there is no motion in the direction of the x - and y - axes. A video of the experiments can also be found by following the following link: <http://youtu.be/BiLiID1MR6o>.

9. CONCLUSION

This paper solves the constrained motion problem for a robotic manipulator by mapping the end-effector velocities to the joint velocities in such a way that the constraints are guaranteed to be satisfied. We solve this at a kinematic level, i.e., we force the velocities in certain directions to vanish in order to avoid hitting

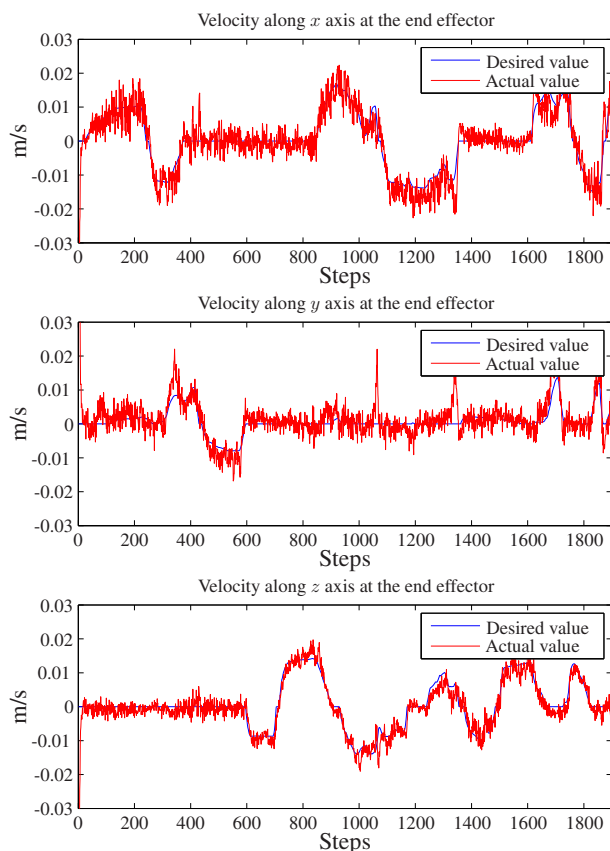


Fig. 4. Linear velocities at the end effector

obstacles. The reduced dimensionality due to the constraints are cast into a reduced velocity space by introducing a new set of velocity variables. The Jacobian is rewritten so that it finds the mapping to the new velocity variables instead of the joint velocities, and as a result the constraints are always satisfied. This mapping is denoted the *Constrained Jacobian Matrix* and presents us with a solution to the inverse kinematics problem for constrained manipulators. Experimental results show the efficiency of the approach.

REFERENCES

A. Abbati-Marescotti, C. Bonivento, and C. Melchiorri. On the invariance of the hybrid position/force control. *J. Intell. Robot. Syst.*, 3(4):233–250, 1990. ISSN 0921-0296.

H. Azimian, R. V. Patel, and M. D. Naish. On constrained manipulation in robotics-assisted minimally invasive surgery. In *Biomedical Robotics and Biomechatronics (BioRob), 2010 3rd IEEE RAS and EMBS International Conference on*, pages 650–655, 2010.

H. Bruyninckx and J. De Schutter. Specification of force-controlled actions in the “task frame formalism”—a synthesis. *IEEE Trans. Robot.*, 12(4):581–589, aug 1996. ISSN 1042-296X.

J. Canny. *The Complexity of Robot Motion Planning*. Acm Doctoral Dissertation Awards, 1987. Mit Press, 1988. ISBN 9780262031363.

J. J. Craig and M. H. Raibert. A systematic method of hybrid position/force control of a manipulator. In *Proc. COMPSAC*

'79, pages 446 – 451, 1979.

P. J. From. On the Kinematics of Robotic-assisted Minimally Invasive Surgery. *Modeling, Identification and Control*, 34 (2):69–82, 2013. doi: 10.4173/mic.2013.2.3.

P. J. From, K. Y. Pettersen, and J. T. Gravdahl. *Vehicle-manipulator systems - modeling for simulation, analysis, and control*. Springer Verlag, London, UK, 2014.

J. Funda, R. H. Taylor, B. Eldridge, S. Gomory, and K.G. Gruben. Constrained cartesian motion control for teleoperated surgical robots. *Robotics and Automation, IEEE Transactions on*, 12(3):453–465, 1996. ISSN 1042-296X.

O. Khatib. Real-time obstacle avoidance for manipulators and mobile robots. *Int. J. Robot. Res.*, 5(1):90–98, 1986.

J. C. Latombe. *ROBOT MOTION PLANNING.: Edition en anglais*. The Springer International Series in Engineering and Computer Science. Springer, 1991. ISBN 9780792391296.

S.M. LaValle. *Planning Algorithms*. Cambridge University Press, 2006. ISBN 9780521862059.

J. Lenarčič and C. Galletti. Kinematics and modelling of a system for robotic surgery. In *On Advances in Robot Kinematics*. Springer, 2004. ISBN 9781402022487.

M. Li, A. Kapoor, and R. H. Taylor. A constrained optimization approach to virtual fixtures. In *Intelligent Robots and Systems, 2005. (IROS 2005). 2005 IEEE/RSJ International Conference on*, pages 1408–1413, 2005.

H. Lipkin and J. Duffy. Hybrid twist and wrench control for a robotic manipulator. *Trans. ASME J. Mech. Transm. Autom. Des.*, 110:138–144, 1988.

R. C. O. Locke and R. V. Patel. Optimal remote center-of-motion location for robotics-assisted minimally-invasive surgery. In *Robotics and Automation, 2007 IEEE International Conference on*, pages 1900–1905, 2007.

T. Lozano-Perez. Spatial planning: A configuration space approach. *Computers, IEEE Transactions on*, C-32(2):108–120, 1983. ISSN 0018-9340.

Matthew T Mason. Compliance and force control for computer controlled manipulators. *Systems, Man and Cybernetics, IEEE Transactions on*, 11(6):418–432, 1981.

C. Natale. *Interaction Control of Robot Manipulators: Six-degrees-of-freedom Tasks*. Springer Tracts in Advanced Robotics. Springer, 2003. ISBN 9783540001591.

C. ODunlaing and C. K. Yap. A retraction method for planning the motion of a disc. *Journal of Algorithms*, 6(1):104 – 111, 1985. ISSN 0196-6774.

T. Ortmaier and G. Hirzinger. Cartesian control issues for minimally invasive robot surgery. In *Proceedings of IEEE/RSJ International Conference on Intelligent Robots and Systems 2000.*, volume 1, pages 565–571 vol.1, 2000.

J. T. Schwartz and M. Sharir. On the piano movers problem i. the case of a two-dimensional rigid polygonal body moving amidst polygonal barriers. *Communications on Pure and Applied Mathematics*, 36(3):345–398, 1983a.

J. T. Schwartz and M. Sharir. On the piano movers problem ii. general techniques for computing topological properties of real algebraic manifolds. *Advances in Applied Mathematics*, 4:298–351, 1983b.

B. Siciliano, L. Sciavicco, L. Villani, and G. Oriolo. *Robotics: Modelling, Planning and Control*. Advanced Textbooks in Control and Signal Processing. Springer, 2011.